FREQUENCY AND TIME SYNCHRONIZATION FOR THE CDMA ARRAY-RECEIVER STAR WITH INTERFERENCE SUBSPACE REJECTION

Besma Smida, Sofiène Affes and Paul Mermelstein

INRS-EMT, Université du Québec
Place Bonaventure, 800, de la Gauchetire Ouest, Suite 6900
Montréal, Québec, H5A 1K6, Canada
Email: smida,affes,mermel@inrs-emt.uquebec.ca

ABSTRACT

This paper investigates the problem of CDMA multi-user detection with STAR-ISR (Spatio-Temporal Array receiver with Interference Subspace Rejection) in the presence of unknown multipath channel and residual carrier offset. We observe that the performance of STAR-ISR could be seriously degraded if no frequency-offset recovery is implemented. We introduce an efficient carrier frequency offset recovery (CFOR) module into STAR-ISR. The proposed CFOR is based on space/time separation that implements a simple linear regression approach for both time-delay and frequency synchronization. We analyze the performance of STAR-ISR with and without CFOR. Simulations show that CFOR reduces the performance loss due to the frequency offset. With frequency offset of 600 Hz the link-level gain is more than 7 dB for 8PSK users.

1. INTRODUCTION

One of the major obstacles in detecting code division multiple access (CDMA) signals is the well-known interference problem. In the past decade, there has been significant interest in multi-user detection. In fact, a variety of receivers that can decouple the superimposed received signals have been investigated [1]. However, most of these previous works assume that there is no carrier frequency offset.

In practical mobile communication scenarios, however, unknown transmission distance will lead to unknown time delay and the carrier frequency may have unknown shift due to oscillator instability and Doppler effect. In a multi-user environment, the frequency offset of one user not only degrades the detection of that user, but also makes the receiver - based on the ideal carrier frequency assumption - no longer optimal, thus degrading the detection of the other users. As shown in [2] the performance of a multi-user detector could be seriously degraded if no frequency offset correction is taken.

In previous work, we proposed a new technique for multi-user detection in CDMA networks [3], denoted Interference Subspace Rejection (ISR). This technique offers different modes that range in performance and complexity between IC (interference cancellation) detectors and linear receivers. Each mode characterizes the interference vector in a different way and accordingly suppresses it. In addition to interference rejection, STAR-ISR performs space and time diversity combining, array processing and time delay synchronization. So far, however, we did not address the problem of carrier-frequency offset recovery in a multi-user detection context.

This contribution incorporates an efficient carrier frequency offset recovery (CFOR) module into the STAR-ISR detector. We propose a new procedure based on space/time separation that implements a simple linear regression approach for estimation of both the time-delays and the frequency offset. This approach was recently validated for single-user receivers [4] where numerical results showed that the new joint time-delay and frequency synchronization algorithm compensates almost completely for the performance loss due to high and low frequency offsets. Implementing this method in a multi-user environment is thus of great interest to increase the robustness of STAR-ISR to the residual carrier offset.

By simulation, we analyze the performance of STAR-ISR with and without CFOR and show that CFOR reduces the performance loss due to the frequency offset. With frequency offset of 600 Hz the link-level gain is more than 7 dB for 8PSK users.

Work supported by Bell/Nortel/NSERC Industrial Research Chair in Personal Communications and by the NSERC Research Grants Program.

2. SYSTEM MODEL

2.1. Data model

We consider an uplink transmission with M receiving antennas at the base station and consider a multipath Rayleigh fading channel with number of paths P and Doppler spread frequency f_D. We also assume a frequency offset Δf due to transmitter and receiver oscillator mismatch. The spreading factor, defined as the ratio between the chip rate and the symbol rate is L. The system consists of U active users. The data for user with index u $b_n^u \in C_K$ is K-PSK modulated at rate $1/T$, where T is the symbol duration and

$$C_K = \{\ldots, e^{\frac{j2\pi k}{K}}, \ldots\},\ k \in \{0, \ldots, K-1\}. \quad (1)$$

The data sequence is then spread by a personal code $c^u(t)$. At time t, the received signal vector from the antenna array can be written as follows:

$$X(t) = \sum_{u=1}^{U} \psi^u(t) X^u(t) + N^{th}(t) \quad (2)$$

$$= \sum_{u=1}^{U} \psi^u(t) H^u(t) \otimes c^u(t) b^u(t) + N^{th}(t), \quad (3)$$

where $X^u(t)$ is the received signal vector from the user u given by the channel response vector $H^u(t)$ from the mobile to the base station spread by $c^u(t)b^u(t)$, $\psi^u(t)$ is the total received amplitude of user u, and $N^{th}(t)$ is the thermal noise received at each antenna element. After pulse matched filtering over a Q symbol duration (i.e. QT), sampling at the chip rate $1/T_c$ and framing over $(Q+1)L$ chip samples at the symbol rate, we obtain the $M \times ((Q+1)L)$ matched-filtering observation matrix [3]:

$$\mathbf{Y}_n = \sum_{u=1}^{U} \psi_n^u \mathbf{Y}_n^u + \mathbf{N}_n^{th} \quad (4)$$

where each user u contributes its user-observation matrix $\mathbf{Y}_n^u$, and where the base-band preprocessed thermal noise contributes $\mathbf{N}_n^{th}$. With respect to the desired user, assigned index d, we can now rewrite the vector-reshaped matched-filtering observation matrix for $k = 0, \ldots, Q-1$ as:

$$\underline{Y}_n = s_n^{d,k} \underline{Y}_n^d + \underline{I}_n + \underline{N}_n, \quad (5)$$

where $s_n^{d,k} = \psi_n^d b_{nQ+k}^d$ denotes the kth signal component of the desired user and $\underline{I}_n$ is part of the multiple access interference (MAI) to be suppressed. The noise vector N_n comprises ISI from the desired user over its kth symbol, the rest of MAI from all other users, and the preprocessed thermal noise.

2.2. Overview of STAR-ISR

In the general case, the total interference $\underline{I}_n$ is an unknown random vector which lies in an interference subspace spanned by a constraint matrix $\mathbf{C}_n$ with dimension depending on the number of interference parameters estimated separately. A number of alternative mode is available to construct the constraint matrix $\mathbf{C}_n$ [5]. In Table I in [3], we show how to form the constraint matrix $\hat{\mathbf{C}}_n$ for different interference subspace characterizations. The TR (total realisation) mode nulls the total interference vector and hence requires accurate estimation of all the channel and data parameters of the NI interferers. The R (realizations) mode nulls the signal vector of each interferer and hence become robust to power estimation errors.

To achieve a near far resistance, the receiver beamformer $\underline{W}_n^{d,k}$ must conform to the following theoretical constraints:

$$\begin{cases} \underline{W}_n^{d,k^H} \underline{Y}_{k,n}^d = 1\,, \\ \underline{W}_n^{d,k^H} \mathbf{C}_n = 0\,, \end{cases} \Rightarrow \begin{cases} \underline{W}_n^{d,k^H} \underline{Y}_{k,n}^d = 1\,. \\ \underline{W}_n^{d,k^H} \underline{I}_n = 0\,. \end{cases} \quad (6)$$

With an estimate of the constraint matrix $\hat{\mathbf{C}}_\mathbf{n}$ made available for a selected mode, we obtain the ISR spatio-temporal beamformer $\underline{W}_n^{d,k}$ by:

$$\mathbf{Q}_n = \left(\hat{\mathbf{C}}_n^H \hat{\mathbf{C}}_n\right)^{-1}, \quad (7)$$

$$\mathbf{\Pi}_n = \mathbf{I}_{N_T} - \hat{\mathbf{C}}_n \mathbf{Q}_n \hat{\mathbf{C}}_n^H, \quad (8)$$

$$\underline{W}_n^{d,k} = \frac{\mathbf{\Pi}_n \underline{\hat{Y}}_{k,n}^d}{\underline{\hat{Y}}_{k,n}^{d^H} \mathbf{\Pi}_n \underline{\hat{Y}}_{k,n}^d}, \quad (9)$$

where $N_T = M(Q+1)L$ is the total space dimension and $\mathbf{I}_{N_T}$ denotes an $N_T \times N_T$ identity matrix. First, we form the projector $\mathbf{\Pi}_n$ orthogonal to the constraint matrix estimate $\hat{\mathbf{C}}_n$. Second, we project the estimated response vector $\hat{\mathbf{Y}}_{k,n}^d$ and normalize it to derive the STAR-ISR combiner. Finally, we extract the signal component by:

$$\hat{s}_n^{d,k} = \underline{W}_n^{d,k^H} \underline{Y}_n\,. \quad (10)$$

3. JOINT TIME-DELAY AND FREQUENCY OFFSET SYNCHRONIZATION

We provide in this section a generalization of the joint time-delay and frequency synchronization procedure, introduced for single-user receivers in [4], to the multi-user case.

The joint synchronization operation for each user u is accomplished in two steps. First, it estimates the number of multipaths $\hat{P}$, their time delays, their relative power and their magnitude. Then, it determines the carrier-frequency

offset. Based on this information an estimate of the spatio-temporal channel is made, and the process is iterated. Key to the present algorithm is the space/time separation procedure that enables us to decouple time and carrier frequency synchronization. The space/time separation has been used in [6] to reduce the identification errors. From the space/time separation (STS) the spatio-temporal channel $\mathbf{H}_n$ can be reconstructed $\hat{\mathbf{H}}_n = \hat{\mathbf{J}}_n \hat{\mathbf{D}}_n^T$ based on estimations of the temporal response matrix $\hat{\mathbf{D}}_n$ and the spatial response matrix $\hat{\mathbf{J}}_n$.

3.1. Time-Delay and Frequency Acquisition

We propose the following algorithm for each user u.

1. Initial multipath detection:

   We estimate $\hat{\mathbf{D}}_n^u$ using the localization spectrum over the possible multipath delays. We limit localization to a simple search over integer multiples of the chip rate (see [7] for more details) to estimate the number of paths $\hat{P}$ and their time-delays.

2. Separation of the spatial response matrix $\hat{\mathbf{J}}_n$:

   Once $\hat{\mathbf{D}}_n^u$ is estimated, we use multi-source beamforming to isolate $\hat{\mathbf{J}}_n^u$ [6]:

   $$\hat{\mathbf{J}}_n^{uT} = (\hat{\mathbf{D}}_n^{uT}\hat{\mathbf{D}}_n^u)^{-1}\hat{\mathbf{D}}_n^{uT}\tilde{\mathbf{H}}_n^{uT}. \quad (11)$$

   The matrix $\hat{\mathbf{J}}_n^u$ is then transformed into an (MP)-dimensional vector $\underline{\hat{J}}_n^u$ by concatenating its columns. We identify its i-th coefficient $\underline{\hat{J}}_{i,n}^u = \hat{r}_{i,n}^u e^{j\hat{\phi}_{i,n}^u}$ by its magnitude $\hat{r}_{i,n}^u$ and its phase $\hat{\phi}_{i,n}^u$.

3. Carrier frequency acquisition:

   We consider a slowly varying channel, which means that channel parameters are unchanged over periods of K symbols while a fixed phase shift (due to carrier offset) is produced between two samples. We buffer, separately, the phase $\hat{\phi}_{i,n}^u$ of each coefficient of $\underline{\hat{J}}_n^u$ with index i (i.e., $\underline{\hat{J}}_{i,n}^u$) over K symbols and apply a LR-based procedure [8] to estimate Δf^u. For each diversity finger for $i = 1, \ldots, MP$, we hence form the following vector:

   $$\hat{\Phi}_{i,nK}^u = [\hat{\phi}_{i,(n-1)K+1}^u, \ldots, \hat{\phi}_{i,(n-1)K+k}^u, \ldots, \hat{\phi}_{i,nK}^u], \quad (12)$$

   then estimate Δf^u at the symbol iteration nK as the slope of a linear regression as follows:

   $$\hat{\Delta} f_{i,nK}^u = \frac{\|R_0\|^2(R_1^T\hat{\Phi}_{i,nK}^u) - (R_1^T R_0)(R_0^T\hat{\Phi}_{i,nK}^u)}{2\pi T\{\|R_0\|^2\|R_1\|^2 - (R_1^T R_0)^2\}}, \quad (13)$$

   where $R_0 = [1, \ldots, 1]$ and $R_1 = [1, \ldots, k, \ldots, K]$. Thus, there are MP estimates of the frequency offset.

   We exploit space-time diversity and minimize estimation errors, by weighted summation over these MP estimates:

   $$\begin{aligned}\hat{\Delta} f_{nK}^u &= \frac{\sum_{i=1}^{MP} \hat{r}_{i,(n-1)K+k}^2 \hat{\Delta} f_{i,nK}^u}{\sum_{i=1}^{MP} \hat{r}_{i,(n-1)K+k}^2} \\ &= \frac{1}{M}\sum_{i=1}^{MP}\left(\frac{\sum_{k=1}^{K} \hat{r}_{i,(n-1)K+k}^2}{K}\right)\hat{\Delta} f_{i,nK}^u. \end{aligned} \quad (14)$$

   For simplicity, we skip the index nK in Δf_{nK}^u in the following step.

4. Reconstruction of the spatio-temporal channel:

   We reconstruct the spatio-temporal propagation vector $\hat{\mathbf{H}}_n^u$ by:

   $$\hat{\mathbf{H}}_n^u = \hat{\mathbf{J}}_n^u \hat{\mathbf{D}}_n^{uT}. \quad (15)$$

We thereby implement a frequency offset acquisition step in a closed loop structure, where we feed back the estimate of the frequency offset to the input of the receiver:

$$\underline{Z}_n^u = e^{-j2\pi\hat{\Delta} f^u nT}(\underline{H}_n^u s_n^u + \underline{N}_n^u). \quad (16)$$

3.2. Time-Delay and Frequency Tracking

1. Tracking the multipath delays:

   We update the time response matrix $\hat{\mathbf{D}}_n^u$ with a subspace-tracking equation:

   $$\tilde{\mathbf{D}}_{n+1}^u = \hat{\mathbf{D}}_n + \frac{\eta}{M}(\hat{\mathbf{H}}_n^{uT} - \hat{\mathbf{D}}_n^u\hat{\mathbf{J}}_n^{uT})\hat{\mathbf{J}}_{n+1}^{u*}, \quad (17)$$

   where

   $$\hat{\mathbf{J}}_{n+1}^{uT} = (\hat{\mathbf{D}}_n^{uT}\hat{\mathbf{D}}_n^u)^{-1}\hat{\mathbf{D}}_n^{uT}\tilde{\mathbf{H}}_{n+1}^{uT}. \quad (18)$$

   We estimate the multi-paths delays with a linear regression, then we rebuild the time-response matrix $\hat{\mathbf{D}}_{n+1}^{uT}$. This step allows the estimation of the spatio-temporal propagation vector $\hat{\mathbf{H}}_{n+1}^u = \hat{\mathbf{J}}_{n+1}^u \hat{\mathbf{D}}_{n+1}^{uT}$.

2. Tracking the frequency offset:

   Similarly to the frequency offset acquisition, we estimate the carrier frequency offset error $\hat{\delta} f_n^u$ by linear regression over successive blocks of length K using the same equations (13) and (14). We update the frequency-offset estimate in equation (15) and (16) as follows:

   $$\hat{\Delta} f_{nK}^u = \hat{\Delta} f_{(n-1)K}^u + \hat{\delta} f_{nK}^u. \quad (19)$$

4. PERFORMANCE ANALYSIS

In this section, we compare and analyze the performance of a previous version of STAR-ISR (with time-delay synchronization only) and STAR-ISR with joint time-delay and frequency synchronization.

4.1. Simulation Setup

We have implemented a link-level simulation of multi-user reception to evaluate the performance of STAR-ISR with CFOR. We considered the uplink of DS-CDMA with a chip rate of 3.840 Mcps operating at a carrier frequency of 1.9 GHz. The spreading factor is $L = 16$ corresponding to a link of 256 Kbaud. The channel is considered Rayleigh fading with Doppler and frequency offset. We assumed frequency selective fading with 3 equal power propagation paths. We considered a delay drift of 0.046 ppm. All the parameters of the channel are varying in time.

The base station has $M = 2$ antennas. We simulated a multirate environment with 6 BPSK users and 6 8PSK users corresponding to transmission rates of 256 Kb/s and 768 Kb/s, respectively. Each user has an individual frequency offset Δf^u with an average equal to Δf. We implemented closed loop power control operating at 1600 Hz and adjusting the power in steps of ± 0.5 dB. An error rate on the power control bit of 5% and a feedback delay of 0.625 ms are simulated.

4.2. Simulation results

In Figures 1 and 2 we show the performance results for STAR-ISR with and without CFOR in terms of BER versus the input SNR after despreading for users of different data-rates using the TR and R modes [3]. In Tab. 1 we also report the SNR required for BER = 5% (BPSK [1]) and BER= 7% (8PSK [2]). Results suggest the following:

- High frequency synchronization errors have a serious impact on the performance of STAR-ISR-TR and STAR-ISR-R. The link level degradation due to $\Delta f = 600Hz$ is particularly severe for 8PSK interferers, more than 9 dB for both STAR-ISR-TR and STAR-ISR-R. In the BPSK case, losses are in the range of 3 dB.

- The link level gain with CFOR is higher for the TR mode than for the R mode. Indeed, the difference between the TR and R modes in SNR requirement, for the same QoS, gets smaller with the introduction of CFOR. The incorporation of CFOR in STAR-ISR makes the TR mode even more attractive, since it presents a better performance/complexity tradeoff [3]. We also notice that the performance gain is higher with 8PSK interferers (more than 7 dB) compared to BPSK users (in the range of 2 dB).

- Comparing the link-level curves of STAR-ISR with CFOR and STAR-ISR with no frequency offset, we notice that CFOR compensates the performance loss due to frequency synchronization errors only partially. This result differs from that of the single-user context where the compensation was almost complete [4]. In a multi-user environment the residual frequency offsets after CFOR, for each user, accumulate in the reconstructed data before suppression (more so on the uplink). This phenomenon makes the complete compensation of the offset difficult to achieve in a multi-user detection context.

	BPSK	8PSK
STAR-ISR-TR without CFOR, Δf =600 Hz	9.75	> 20
STAR-ISR-TR with CFOR, Δf =600 Hz	7.25	9.75
STAR-ISR-TR ,Δf =0 Hz	6.75	7.5
STAR-ISR-R without CFOR, Δf =600 Hz	8.25	16
STAR-ISR-R with CFOR, Δf =600 Hz	6.25	9
STAR-ISR-R ,Δf =0 Hz	5.5	7

Table 1. Required SNR in dB for BPSK and 8PSK users.

5. CONCLUSION

In this contribution we incorporated an efficient carrier frequency offset recovery module into STAR-ISR detector. This procedure implements simple linear regression for both frequency and time-delay synchronization. The simulations show that CFOR reduces the performance loss due to the frequency offset. With a frequency offset of 600 Hz the link-level gain is more than 7 dB for 8PSK users. Current investigations address extension of the proposed joint time-delay and frequency synchronization with STAR-ISR to future multi-carrier air interfaces.

[1] A BER = 5% before FEC decoding is equivalent to a BER=10^{-5} after decoding.

[2] A BER = 7% before FEC decoding is equivalent to a BER=10^{-5} after decoding.

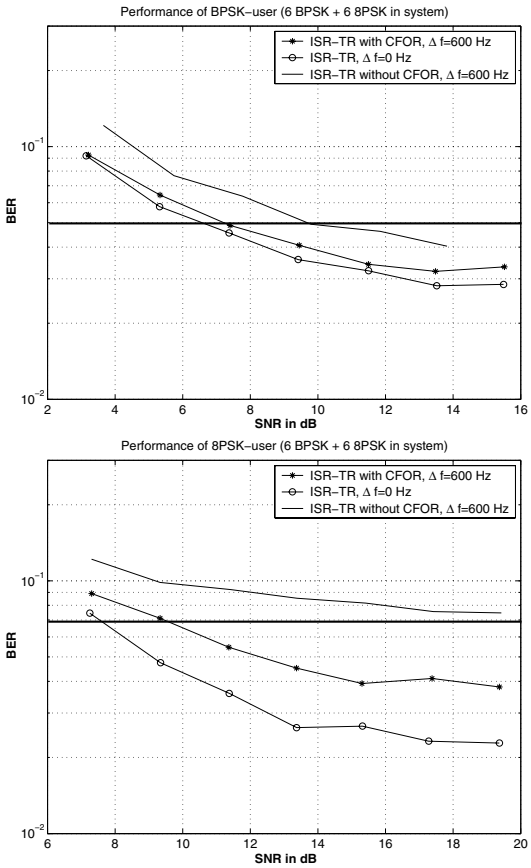

Fig. 1. BER versus SNR for STAR-ISR-TR with and without CFOR (a) BPSK (b) 8PSK.

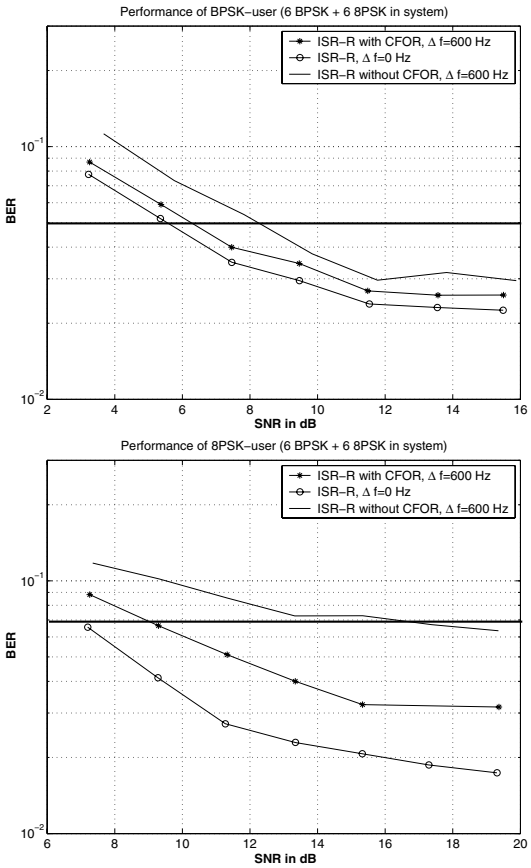

Fig. 2. BER versus SNR for STAR-ISR-R with and without CFOR (a) BPSK (b) 8PSK.

6. REFERENCES

[1] S. Verdu, *Multiuser Detection*, Cambridge, UK: Cambridge Univ. Press, 1998.

[2] F.-C. Zheng and S. K. Barton, "On the performance of near/far resistant CDMA detectors in the presence of synchronization errors", *IEEE Trans. Commun.*, vol-43, pp.3037-3045, Dec. 1995.

[3] S. Affes, H. Hansen, and P. Mermelstein, "Interference subspace rejection : a framework for multiuser detection in wideband CDMA", *IEEE Journal on Selected Areas in Communications*, vol. 20, no. 2, Feb. 2002.

[4] B. Smida, S. Affes, and P. Mermelstein, "Joint time-delay and frequency offset synchronization for CDMA array-receivers" to appear *SPAWC 2003*, Rome, Italy.

[5] S. Affes, H. Hansen, and P. Mermelstein, "Interference subspace rejection in wideband CDMA: modes for mixed-power operation", *Proc. of IEEE ICC'01, Communication Theory Symposium*, Helsinki, Finland, vol. 2, pp. 523-529, June 11-15, 2001.

[6] S. Affes, P. Mermelstein, "A new receiver structure for asynchronous CDMA: STAR-the spatio-temporal array-receiver", *IEEE J. Select. Areas in Comm.*, vol. 16, no. 8, pp. 1411-1422, October 1998.

[7] K. Cheikhrouhou, S. Affes, and P. Mermelstein, "Impact of synchronization on performance of enhanced array-receivers in wideband CDMA networks", *IEEE J. Select. Areas in Comm.*, vol. 19, no 12, pp. 2462-2476, December 2001.

[8] S. Affes, J. Zhang, and P. Mermelstein, "Carrier frequency offset recovery for CDMA array-receivers in selective Rayleigh-fading channels", *proc. of 55th IEEE VTC'2002*, Vol. 1, pp. 180-184. Birmingham, USA.